Titan's Gravity Well

January 2021

The competition surface for the 2022 Cassani Mission MECH223 design project incorporates a funnel feature that simulates the gravity well of Titan. The behavior of the 'landers' inside the confines of the funnel is one of the larger unknown factors in the analysis of the design problem. Constructing an analytical model of the behavior and motion of a small mass traveling across the funnel surface can help us determine the optimal entry conditions for a lander into Titan's gravity well. The goal of the competition is to maximize the time required to travel from the top of the funnel to the bottom.

The competition funnel is radially symmetric and can be modeled by a function relating the vertical distance from the competition table and the radius from the center of Titan as follows:

$$z(r) = \begin{cases} -\frac{r^2-0.913r+0.209}{4.93r^2+r+0.36} & 0.15\text{m} \leq x \leq 0.45\text{m} \\ \\ -0.457+2.03r & x < 0.15\text{m} \end{cases}$$

In analysing the lander behavior for a small ball, it is most helpful to treat it as a point mass. As the radius of the small lander ball approaches zero, the angular momentum of the ball also approaches zero and the approximation becomes more and more accurate. The full analysis of the mechanics of a rolling ball, and the complexities of variable slipping and non-slipping contact with the funnel surface is a topic too advanced to attempt in the time constraints of the MECH223 competition. For our purposes and for small external torques on the rolling lander, such as on a smooth competition surface, we can use this approximation. Furthermore, the lander should behave as though its inertial mass has increased in proportion to its moment of inertia when using this method, see (English et. al, 2012). With these considerations in mind, we can examine further the case of a solid ball.

Due to the radial symmetry of the problem, it is most helpful to work in cylindrical coordinates centered on the center of Titan. As a refresher for those who are not familiar with this coordinate system, the position vector $\vec{P}$ of the lander is described by an angle, a radius, and a height measured from the origin, see Figure 1 below.

In this configuration we have the relationships:

$$\begin{aligned} x &= r\cos\theta \\ y &= r\sin\theta \\ r^2 &= x^2+y^2 \\ \theta &= \arctan(y/x) \end{aligned}$$

To begin our model, we first consider the case without any sliding friction on the ball, which is a reasonable approximation. The rolling ball has a contact point with the surface which produces a static friction. However, recall that there is an ICZV at the point of contact with the surface, such that there is no work done on the ball by friction. $W = Fd$ where $d = 0$. The radial symmetry of

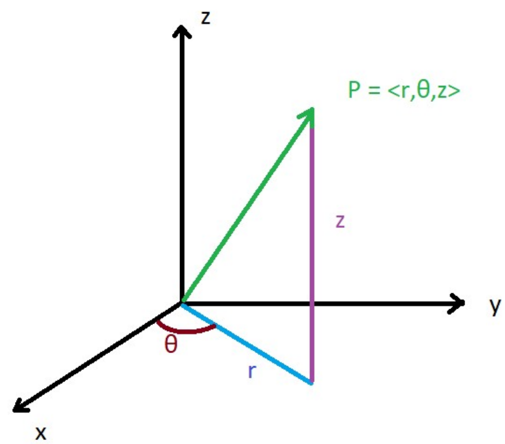

Figure 1: Relationship of Cartesian and Cylindrical Coordinates

the funnel ensures that the normal force vector is always directed towards the z-axis, revealing an important conclusion about the system. There are no forces acting in the θ direction on the mass, and so in the absence of friction, the angular momentum of the lander is constant.

$$mr^2\dot{\theta} = L = \text{constant} \tag{1}$$

$$\implies \dot{\theta} = \frac{L}{mr^2} \tag{2}$$

$$\tag{3}$$

As the ball approaches the z-axis, it will rotate faster about the axis, which will oppose the tendency of the ball to fall down into the center of the funnel due to gravity. We can examine a generalized case of a small mass treated as a point on a sloped surface in a coordinate system anchored on the mass with acceleration forces directed in the z, θ, and r axes. The equations of motion for this configuration are given as:

$$\sum F_z = ma_z = m\ddot{z} \tag{4}$$

$$\sum F_\theta = ma_\theta = m(r\ddot{\theta} + 2\dot{r}\dot{\theta}) \tag{5}$$

$$\sum F_r = ma_r = m(\ddot{r} - r\dot{\theta}^2) \tag{6}$$

The dot notation signifies a time derivative, which will be mixed in with other types of derivatives in the analysis ahead. The ball is constrained to the surface of the funnel by gravity as long as the vertical acceleration does not exceed the acceleration due to gravity. For the normal operation conditions of lander deployment we will be focused on the case where the lander stays in contact with the surface. $\ddot{z}$ is derived as follows:

$$z = z(r(t)) \tag{7}$$

$$\dot{z} = \frac{dz}{dr} \cdot \frac{dr}{dt} \qquad \text{Chain Rule} \tag{8}$$

$$\ddot{z} = \frac{d^2z}{dr^2}\dot{r}^2 + \frac{dz}{dr}\ddot{r} \qquad \text{Product and Chain Rule} \tag{9}$$

The derivatives $\frac{d^2z}{dr^2}$ and $\frac{dz}{dr}$ have not been shown as the explicit solutions are very long for the outer funnel function. They can be derived using first-principles of differential calculus.

Consider a small mass on an inclined slope with no work done by friction in Figure 2 below. By equations (4-6) above we sum the forces as follows:

$$\sum F_z = ma_z = m\ddot{z} = N\cos(\phi) - mg \tag{10}$$

$$\sum F_\theta = ma_\theta = m(r\ddot{\theta} + 2\dot{r}\dot{\theta}) = 0 \tag{11}$$

$$\sum F_r = ma_r = m(\ddot{r} - r\dot{\theta}^2) = -N\sin(\phi) \tag{12}$$

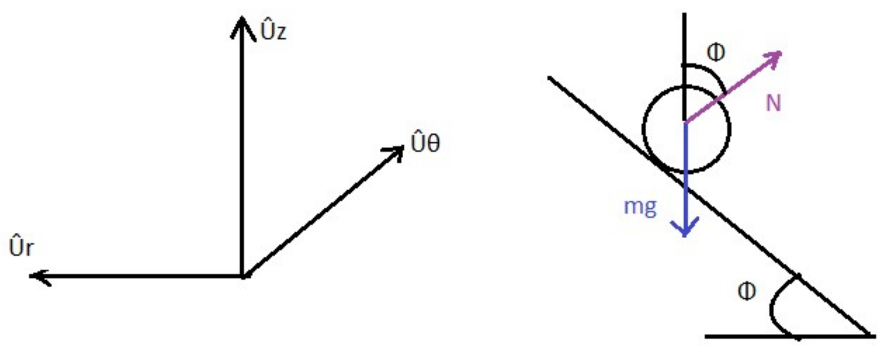

Figure 2: Free Body Diagram and Linear Relative Coordinates

We can make a series of steps to further reduce the problem into a system of differential equations as follows:

$$(11) \implies r\ddot{\theta} + 2\dot{r}\dot{\theta} = 0 \tag{13}$$

$$\ddot{\theta} = -2\frac{\dot{r}\dot{\theta}}{r} \tag{14}$$

$$(10) \implies N\cos(\phi) = m\ddot{z} + mg \tag{15}$$

$$(12) \implies -N\sin(\phi) = m(\ddot{r} - r\dot{\theta}^2) \tag{16}$$

$$(15,16) \implies -\tan(\phi) = \frac{\ddot{r} - r\dot{\theta}^2}{\ddot{z} + g} \qquad \text{(16)/(15) division} \tag{17}$$

$$-\frac{dz}{dr} = \frac{\ddot{r} - r\dot{\theta}^2}{\ddot{z} + g} \qquad \text{Slope is the derivative} \tag{18}$$

$$\frac{dz}{dr}(\ddot{z} + g) = r\dot{\theta}^2 - \ddot{r} \tag{19}$$

$$\frac{dz}{dr}\ddot{z} + \ddot{r} = r\dot{\theta}^2 - \frac{dz}{dr}g \tag{20}$$

$$(9) \implies \frac{dz}{dr}\left(\frac{d^2z}{dr^2}\dot{r}^2 + \frac{dz}{dr}\ddot{r}\right) + \ddot{r} = r\dot{\theta}^2 - \frac{dz}{dr}g \tag{21}$$

$$(21) \implies \ddot{r} = \frac{1}{1 + \frac{dz}{dr}^2}\left(r\dot{\theta}^2 - \frac{dz}{dr}\left(g + \frac{d^2z}{dr^2}\dot{r}^2\right)\right) \tag{22}$$

Equations (14) and (22) form a system of differential equations that can be further reduced into a system of first order equations:

$$\begin{bmatrix} \ddot{r} \\ \dot{r} \\ \ddot{\theta} \\ \dot{\theta} \end{bmatrix} = \begin{bmatrix} \dot{r} \\ r \\ \dot{\theta} \\ \theta \end{bmatrix}' = \begin{bmatrix} \frac{1}{1+\frac{dz}{dr}^2}\left(r\dot{\theta}^2 - \frac{dz}{dr}\left(g + \frac{d^2z}{dr^2}\dot{r}^2\right)\right) \\ \dot{r} \\ -2\frac{\dot{r}\dot{\theta}}{r} \\ \dot{\theta} \end{bmatrix} \tag{23}$$

Equation (23) can be numerically analysed using a computer assisted solver such as ode45. Explicit solutions do exist if we use constant conservation of angular momentum, in which $\dot{\theta}$ becomes a function of r. In this case, the path trajectory purely in terms of r can be calculated via a second order differential equation for r, and the other two cylindrical coordinates of θ, z can be solved using the functional dependencies. Namely, $\dot{\theta}(r) = \frac{L_0}{mr^2}$ where L_0 is the initial angular momentum at entry into the funnel. The integral is taken of both sides in this case to solve for $\theta(r)$. For the case of $z(r)$ it is simply the piece wise function describing the funnel surface.

The benefit of the larger system of equations in (23) is that friction forces can be applied. The frictionless case has highly symmetrical behavior where the energy of the lander is always conserved. Large speeds are attained as it approaches $r = 0$ causing it to launch out of the funnel in an unrealistic manner, see some of the figures in (English et. al, 2012).

Friction can be added to the system by assuming that the friction and drag forces on the ball resemble rolling friction with a small coefficient. The direction of friction is always in the opposite direction of the velocity, which is represented by the negative unit vector of velocity. The magnitude is a function of the normal force, combining these two:

$$\hat{\mathbf{v}} = \frac{[\dot{r}, r\dot{\theta}, \dot{z}]}{\sqrt{\dot{r}^2 + (r\dot{\theta})^2 + \dot{z}^2}} \tag{24}$$

$$\vec{F_f} = -\mu N \hat{\mathbf{v}} \tag{25}$$

The previously solved system of equations of motion becomes more complex as follows:

$$\sum F_z = ma_z = m\ddot{z} = N\cos(\phi) - mg - \mu N\hat{\mathbf{v}}_z \tag{26}$$
$$\sum F_\theta = ma_\theta = m(r\ddot{\theta} + 2\dot{r}\dot{\theta}) = -\mu N\hat{\mathbf{v}}_\theta \tag{27}$$
$$\sum F_r = ma_r = m(\ddot{r} - r\dot{\theta}^2) = -N\sin(\phi) - \mu N\hat{\mathbf{v}}_r \tag{28}$$

$$\vec{N} + \vec{F_g} + \vec{F_f} = m\vec{a} \tag{29}$$
$$\vec{N} + \vec{F_g} = m\vec{a} \qquad \vec{F_f} << \vec{N} \tag{30}$$
$$\vec{N} = m(\vec{a} + [0, 0, g]) \tag{31}$$
$$N = m\sqrt{a_r^2 + a_\theta^2 + (a_z + g)^2} \tag{32}$$

We can approximate N in a given state now. The accelerations in the unit directions can be determined by using the original equations of motion given in Equations (4-6), since we have previously calculated the frictionless case for all RHS elements in those equations. In turn the acceleration components are used to solve for N. Finally we can resolve using a second iteration with friction for the altered values of $\ddot{\theta}$ and $\ddot{r}$:

$$(27) \implies \ddot{\theta} = \frac{1}{r}(\frac{-\mu N\hat{\mathbf{v}}_\theta}{m} - 2\dot{r}\dot{\theta}) \tag{33}$$
$$(28) \implies \ddot{r} = \frac{1}{m}(-N\sin(\phi) - \mu N\hat{\mathbf{v}}_r) + r\dot{\theta}^2 \tag{34}$$
$$\sin(\phi) = \frac{\frac{dz}{dr}}{\sqrt{1 + \frac{dz}{dr}^2}} \tag{35}$$

The final equation for $\sin(\phi)$ is determined by the property that $\tan(\phi) = \frac{dz}{dr}$, so solving for $\sin(\arctan(\frac{dz}{dr}))$.

In this case there is no access to the modeled funnel for testing predicted behavior, although some past competition footage can confirm some of the desired entrance velocities and orbit patterns. The system of equations and iterative methods described above have been employed in a MatLab simulation. A value of roughly $\mu = .04$ gives some promising trajectories. Further analysis of the system would likely show that friction forces more complex than rolling friction are at play. Particularly, it seems as though the elements of friction in the z and r directions might be characteristically different due to the the ball being a rolling object and not a point mass. See Figure 3 below for a sample trajectory.

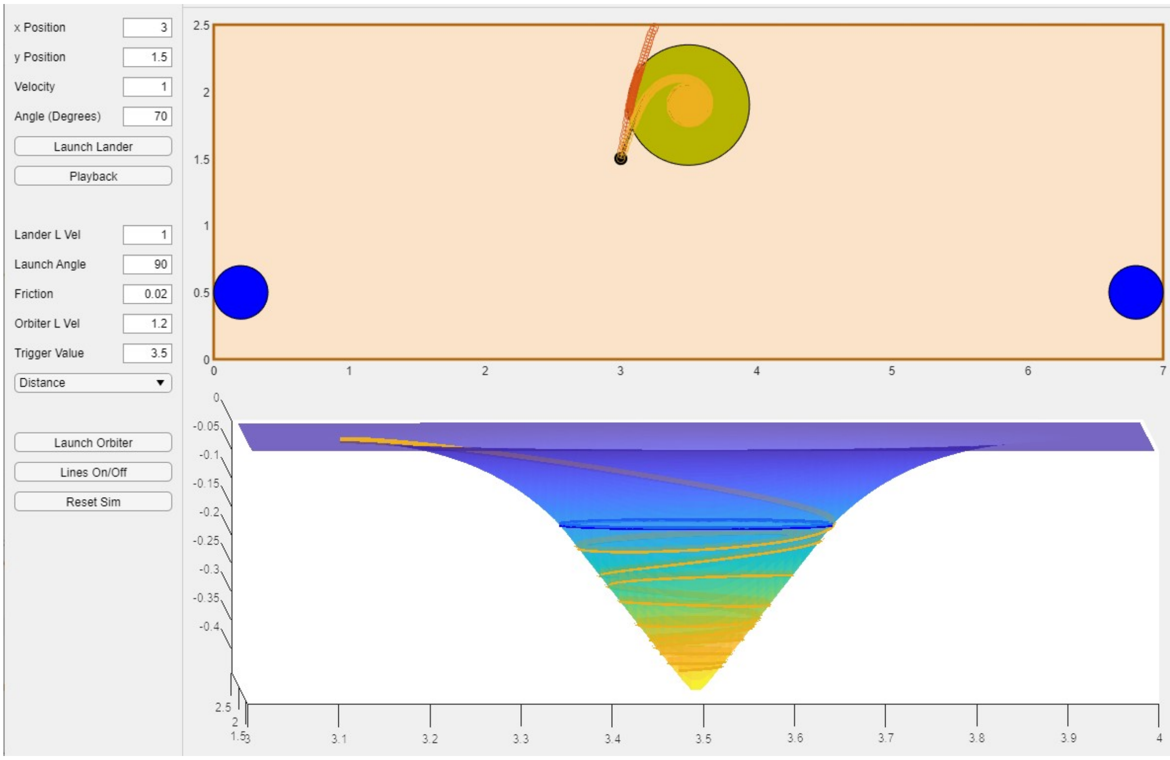

Figure 3: Simulated Trajectory

English, Lars Q., and A. Mareno. "Trajectories of Rolling Marbles on Various Funnels." American Journal of Physics 80, no. 11 (2012): 996-1000.

Math 1302, Week 4: Motion on a surface in 3D - UCL. (n.d.). Retrieved January 25, 2022, from https://www.ucl.ac.uk/ ucahad0/1302week45surf_rev.pdf